The thyroid hormone inactivator enzyme, Type 3 deiodinase, is essential for coordination of keratinocyte growth and differentiation

Giuseppina Mancino[1], Annarita Sibilio[1], Cristina Luongo[2], Emery Di Cicco[1], Caterina Miro[2], Annunziata Gaetana Cicatiello[1], Annarita Nappi[2], Serena Sagliocchi[1], Raffaele Ambrosio[3], Maria Angela De Stefano[1], Daniela Di Girolamo[1], Feliciano Visconte[4] and Monica Dentice[1, 4]♯

[1]Department of Clinical Medicine and Surgery, University of Naples "Federico II", Naples, Italy; [2]Department of Public Health, University of Naples "Federico II", Naples, Italy; [3]IRCCS SDN, Naples, Italy; [4]CEINGE–Biotecnologie Avanzate Scarl, Naples, Italy;

♯ Correspondence: monica.dentice@unina.it

Running Title: Thyroid hormone regulates epithelial homeostasis.

The authors have declared no conflict of interest

Abstract

Thyroid hormones (THs) are key regulators of development, tissue differentiation and maintenance of metabolic balance in virtually every cell of the body. Accordingly, severe alteration of TH action during fetal life leads to permanent deficits in humans. The skin is among the few adult tissues expressing the oncofetal protein type 3 deiodinase (D3), the TH inactivating enzyme. Here, we demonstrate that D3 is dynamically regulated during epidermal ontogenesis. To investigate the function of D3 in a post-developmental context, we used a mouse model of conditional epidermal-specific D3 depletion. Loss of D3 resulted in tissue hypoplasia and enhanced epidermal differentiation in a cell-autonomous manner. Accordingly, wound healing repair and hair follicle cycle were altered in the D3-depleted epidermis. Furthermore, *in vitro* ablation of D3 in primary culture of keratinocytes indicated that various markers of stratified epithelial layers were up-regulated, thereby confirming the pro-differentiative action of D3 depletion and the consequent increased intracellular T3 levels. Notably, loss of D3 reduced the clearance of systemic TH in vivo, thereby demonstrating the critical requirement for epidermal D3 in the maintenance of TH homeostasis. In conclusion, our results show that the D3 enzyme is a key TH-signaling component in the skin thereby providing a striking example of a physiological context for deiodinase-mediated TH metabolism, as well as a rationale for therapeutic manipulation of deiodinases in patho-physiological contexts.

Introduction

The skin protects organisms from infection, prevents dehydration, and undergoes re-epithelialization after wound injury (1). In mammals, epidermal development is a multistage process consisting of epidermal specification, commitment, stratification and terminal differentiation (1). To accomplish these feats, the epidermis constantly replenishes itself thanks to the presence of stem cells that are capable of self-renewal and of producing transiently amplifying progenitor cells. Dividing cells in the innermost (basal) epidermal layer continually execute a program of terminal differentiation, move outwards, exit the cell cycle and embark on a terminal differentiation pathway as they migrate toward the skin surface (1). During the whole process, distinct signaling patterns specify different developmental stages and these stage-specifically regulated signaling events ensure the correct morphogenesis of skin epidermis and its appendages (2). Basal layer keratinocytes express the keratins K5 and K15. As cells exit from the basal layer and begin their journey towards the skin surface, they cease expressing K15 and K5 and start expressing K1 and K10 (3), (4). The first suprabasal cells are known as "spinous cells", which reflects their cytoskeleton of K1/K10 filament bundles connected to robust cell–cell junctions known as "desmosomes". K6, K16 and K17 are also expressed suprabasally, but only in hyperproliferative situations such as wound healing (3), (4).

The skin is a well-recognized target of TH, which is an important regulator of epidermal homeostasis (5). In skin, TH exerts profound effects on fetal epidermal differentiation, barrier formation, hair growth, wound healing, keratinocyte proliferation, and keratin gene expression (6). Moreover, several TH responsive genes have been identified in skin. For example, TH differentially regulates the K5, K14, and K17 gene promoters and the hairless gene (Hr) is a well known TH-target gene in keratinocytes (7).

Although various studies have provided insights into how TH regulates specific stages of epidermal homeostasis (8), (9) few have examine the effects of an altered TH signal at cell-specific level, and the consequence of imbalanced TH homeostasis in physiological conditions.

Three selenoenzymes, namely deiodinases, play a crucial role in the control of TH intracellular availability. These enzymes metabolize THs in a stage- and tissue-specific

manner by a mono-deiodination reaction that involves two distinct pathways. The type 1 and 2 deiodinases (D1 and D2) catalyze the conversion of the inactive precursor T4 to the active form T3 — a process that increases circulating T3 levels and the availability of the active hormone for the nuclear receptors (10). In contrast, type 3 deiodinase (D3) inactivates TH by converting T4 and T3 to the inactive metabolites reverse T3 (rT3) and T2, respectively. Notably, the combined actions of D2 and D3 are viewed as a cell autonomous pre-receptoral mechanism that controls TH signalling in a time- and tissue-specific manner although it does not affect serum hormone concentrations (10), (11)

D3 —- the main physiologic inactivator of TH —controls TH homeostasis by protecting tissues from an excess of TH (12). It is abundantly present in fetal tissues and high D3 levels are expressed in the human placenta, where it blocks the excessive maternal-to-fetal transfer of T4 (13). In contrast, during late neonatal and adult life, D3 expression is more limited in only a number of postnatal tissues, i.e., skin and brain, and in pregnant uterus (14). Notably, D3 is expressed in several pathophysiological conditions, among which cardiac hypertrophy, chronic inflammation, critical illness (15), hypoxia, ischemia (16) and cancer. We and others demonstrated that D3 is up-regulated in basal cell carcinoma, (17) colon carcinoma (18), hemangiomas (19), astrocytomas and glioblastomas (20). Because D3 is expressed in fetal and in malignant tissues, it is referred to as an “oncofetal enzyme”.

Despite evidence that TH plays an important role in epidermal proliferation, the physiologic role of TH and its local modulation by D3 in skin is not well understood. Here, we investigated the physiological role of D3 in the maintenance of the proliferation/differentiation balance of keratinocytes. *In vitro* and *in vivo* experiments demonstrated that epidermal depletion of D3 dramatically alters the proportion of the epithelial layers, thus resulting in a drastic reduction of the skin thickness. Loss of D3 in the epidermis, by reducing the percentage of epidermal stem cells, impairs a correct closure of the wound after an injury and alters the execution of the hair follicle cycle. Notably, the clearance of T4 is reduced in the absence of D3 in the skin, thus revealing a critical role for D3 in the homeostatic control of local and systemic TH levels.

Results

Endogenous type 3 deiodinase is dynamically expressed during epidermal development and the hair follicle cycle.

To assess the localization of D3 during epidermal development and in adult skin, we analyzed its expression in during mouse embryogenesis (E11.5 to E18.5). We found that D3 expression starts at E15.5, peaks at E17.5, and declines thereafter (Figure S1). As shown in Figure 1A-C, D3 expression is highly dynamic in early post-natal life. In fact, it is much lower at P2 than during embryogenesis. It peaks at P10, decreases thereafter, and reaches a plateau in adult life (Figure 1A-C). Immunofluorescence analysis showed that D3 localizes in all the epidermal layers (Figure 1A), and is expressed also in hair follicles mainly at P10, where it reaches its highest levels. Interestingly, this profile positively correlates with miR21 expression and negatively with GRHL3 expression (Figure 1D), both of which have been shown to coordinately regulate D3 expression in skin (21). During the hair follicle cycle, D3 is highly expressed at anagen and catagen, declining in telogen (Figure 1E, F). To assess the specific localization of D3 in the hair follicle, we analyzed the profile of D3 protein expression in the adult epidermis. Immunohistochemical analysis showed that D3 is highly expressed in the bulge region and in sebaceous gland of the hair follicle and is absent in the dermal papilla. D3 was also detected in infundibulum cells and in the interfollicular epidermis (Figure S2). Collectively, these results indicate that in normal epidermis, D3 is dynamically expressed in the epidermal layers of the skin and its expression correlates with hair follicle formation. Intriguingly, in normal skin, D3 expression correlates with of miR-21/GRHL3, suggesting the existence of a regulatory cascade in the control of epidermal homeostasis.

Spatiotemporal D3 genetic depletion accelerates basal cell differentiation.

To investigate the functional role of D3 in epithelial homeostasis, we generated an animal model for epidermal D3 loss of function. To deplete D3 in the epidermis, mice in which the *Dio3* gene is flanked by Lox-P sequences (22) were crossed with transgenic mice with keratinocyte-specific expression of a Cre^{ERT} recombinase under the control of the keratin 14 (K14) promoter (Figure S3A-C) that is responsible for ubiquitous recombination in hair follicles and basal cells of epidermis (23). Because D3

147 expression is dynamically regulated during ontogenesis (Figure 1A), we depleted D3 at
148 day P6, before the massive induction of D3 in the epidermis (Figure 2A). Loss of D3 in
149 the epidermal layers resulted in reduced skin thickness (Figure 2B-G). Indeed, the
150 number of EdU-positive cells and the expression of the proliferative marker K6 and the
151 basal marker K5 were lower in the epidermis of D3KO mice than in control mice
152 (Figure 2B, F and Figure 2C-E). Interestingly, Loricrin, which marks the most
153 differentiative layers in the control mice, was higher in D3KO mice and localized not
154 only in the upper layers as in the control mice, but also in the lower epidermal layers
155 (Figure 2C). Together with the fewer EdU-positive cells and reduced thickness, these
156 data are indicative of the accelerated differentiation of the keratinocytes in the D3KO
157 epidermis.
158 Since the basal layer marker K5 is reduced in D3KO mice, we asked whether D3
159 also affects the stem cell compartment. Therefore, we measured the percentage of
160 $CD34^+$ stem cells by FACS analysis (α6-$Integrin^+/CD34^+$ cells). As shown in Figure 2H,
161 the number of $CD34^+$ cells were much lower in the D3KO epidermis than in control
162 mice (Figure 2H).
163 To perform lineage tracing, we crossed D3KO mice with the double fluorescent
164 Tomato/GFP mouse. Consistent with the hypothesis that excessive T3 exposure
165 induces premature differentiation of keratinocytes in D3KO mice, we observed that
166 while control mice expressed green cells in both basal and suprabasal layers, as
167 expected by the normal replenishment model of basal keratinocytes, green cells
168 produced by Cre-mediated Tomato-GFP shift in the D3KO mice moved rapidly to the
169 upper layers and at day 15 after recombination, were located only in the outer epidermis
170 (Figure 2I). These data show that alteration of the thyroid status by reduced expression
171 of D3 induces deregulation of epidermal homeostasis and support a model in which
172 enhanced T3 in D3KO epidermis induces keratinocyte differentiation (Figure 2L).
173
174 **D3 depletion and thyroid hormone treatment increases keratinocyte differentiation**
175 ***in vitro***
176 The epidermal *in vivo* alterations observed may reflect a direct role of D3 and TH in
177 keratinocyte growth/differentiation control. To test the effects of D3 depletion or T3-
178 treatment in the control of the differentiation/proliferation balance, we used primary

cultures of keratinocytes. We first observed that D3 is expressed in freshly isolated keratinocytes and that its expression declines during the differentiation induced by increased Ca^{2+} concentration in the medium (Figure 3A). D3 was then depleted in primary keratinocytes from D3KO mice infected with an adenovirus carrying the CRE (Ad-CRE) recombinase or with an adeno-GFP (Ad-GFP) virus as control. Loss of D3 caused a reduction in cell proliferation in D3-depleted cells measured by BrdU incorporation (Figure 3B, C). Accordingly, mRNA expression of cyclin D1 and K14 were reduced while the expression of differentiation markers K10 and involucrin was up-regulated (Figure 3D). Furthermore, D3 depletion induced an alteration of keratinocyte morphology. Indeed, as shown in Figure 3E, keratinocytes were smaller and round, which suggested spontaneous, early differentiation (Figure 3E).

To investigate the differentiation potential of D3KO keratinocytes, we induced cell differentiation by Ca^{2+} treatment and measured various differentiation markers, namely, K1, loricrin, Pvrl4 (a cell adhesion molecule mainly implicated in the formation of cadherin-based adherens junctions (24)) and desmoglein 1 (Dsg1, an epidermal adhesion molecule (25)) in AdCRE and AdGFP infected keratinocytes. All these markers were up-regulated in D3-depleted keratinocytes compared to control keratinocytes (Figure 3F), which confirms that local TH excess drives the cells towards functional differentiation. Treatment with 30 nM T3 paralleled the effects of D3 depletion in a time-dependent manner, with reduction of cyclin D1 and K14 and up-regulation of K10 and involucrin (Figure 3G).

Wound healing repair is delayed and hair follicle cycle is accelerated in D3KO skin.

Having ruled out defects in epithelial commitment and differentiation in epithelia lacking D3, we evaluated the ability of D3KO mice to repair the skin damage induced by a wound. We first examined the expression patterns of D3 after the wound created in the dorsal skin in mice. Three days after full-thickness injury, expression levels of D3 mRNA and protein increased significantly, reached a peak at day 6, and declined thereafter (Figure 4A, B). Compared to the control mice, D3KO mice exhibited a sharp delay in their regenerative ability as demonstrated by increased wound area and a delay

in the wound closure (Figure 4C, D). Indeed, while in control mice wound areas were smaller with linear kinetics during the 8-dayperiod of observation, at the end of which ~95% closure was observed, wound closure was significantly delayed in D3KO mice, which showed a 60% wound closure at day 6 and only 70% wound closure at day 8 (Figure 4D).

Histological examination confirmed the delay in skin regeneration, as showed by the absence of epidermic patch in D3KO skin at day 8 post-injury in contrast to the formation of the normal epidermal layer under the scar in control skin (Figure 4E). We speculated that this phenotype could be due to a proliferative defect of D3KO keratinocytes. Indeed, mRNA levels of cyclin D1and K5 were lower in the D3KO epidermis than in control mice (Figure 4F). Moreover, there were fewer $BrdU^+$ nuclei in the zone surrounding the wound in D3-depleted skin than in control mice (Figure 4G, H).

Loss of D3 induces premature involution to telogen during hair follicle cycle.

Given that D3 expression is up-regulated during anagen (Figure 1D, F), we asked if also the hair follicle cycle is affected by D3 depletion. Consequently, as shown in Figure 5A, D3 was depleted in 3-month-old mice by tamoxifen treatment and one week later mice were shaved by clamp and the progression of the hair cycle was assessed 6 (anagen), 10 (catagen) and 30 days (telogen) thereafter. Interestingly, while hair morphology was normal in D3KO mice in anagen, hair bulbs were narrower and hair length shorter in catagen, which indicates premature involution of the follicle to the telogen phase and altered evolution of the hair follicle (Figure 5B, C). In line with the premature catagen-telogen transition, the expression of telogen markers (Hand2, Sox1, ZEB1 and ZEB2, (26) were up-regulated in the D3KO mice already when control hairs were in catagen (Figure 5E), while the anagen markers (Dlx3, FoxN1, K35 and K32, (26)) were unchanged or sharply up-regulated in D3KO mice compared to control mice (Figure 5D).

These data are in accordance with a premature differentiation of the hair follicle cycle cells induced by D3 depletion.

Epidermal D3 expression plays a central role in thyroxine clearance

Since D3 is expressed in adult mice only in brain and skin, and considering that the skin is the largest organ of the body, we wondered whether epidermal D3 might play a role in systemic thyroxine clearance. To this aim, we measured the levels of D3 in the skin of control mice and mice in which we intraperitoneally injected a supraphysiological dose (20 μg/100g weight) of T4 for 3 and 7 days. As shown in Figure 6A, B, D3 expression was up-regulated in hyperthyroid mice, thereby confirming the homeostatic feedback regulation of TH inactivating enzyme by its substrate. Next, we intraperitoneally injected a supraphysiological dose of T4 and evaluated T4 clearance in D3KO mice and control mice by measuring the systemic levels of T4 in the blood at 24 and 48 hours after injection. Notably, the ability to metabolize T4 was sharply reduced (40% at 24 hours and of about 33% at 48 hours) in D3KO mice versus control mice (Figure 6C). These results revealed a new role of epidermal D3 in the regulation of plasma TH concentrations.

Discussion

Mouse epidermis is an attractive model system with which to study the control of epithelial cell growth and differentiation (27). Thyroid hormone is important for the development of many tissues, and in adults regulates the balance between proliferation and differentiation of virtually every cell of the body (28), (29). Thyroid hormone is a key regulator of epidermal proliferation and differentiation, hair growth, and wound healing in humans (8) and mice (5), (30). A striking example is given by the amphibian metamorphosis, during which TH governs various differentiation programs including the switch from a bilayered non-keratinized epithelium to a stratified, keratinized epidermis (31).

Hyperthyroidism in humans leads to alterations in the skin homeostasis and increases perspiration, heat, urticaria, vitiligo, and enhanced pigmentation (32). Notably, the epidermis is thinner in hyperthyroid patients than in euthyroid subjects (32). On the contrary, hypothyroidism is associated with a dry, cold and rough epidermis, with signs of hyperkeratosis, alopecia and sometime diffuse myxedema (32).

Although the effects of thyroid alterations on skin homeostasis have been widely described, the molecular mechanisms by which TH influences keratinocyte turnover and differentiation are still poorly understood. The effects of TH on keratinocyte dynamics are mostly exerted through transcriptional regulation mediated by the genomic action of the two TH nuclear receptors, TRα and TRβ, which act both as positive or negative regulators of transcription on different promoters and in different pathophysiological conditions (10).

The novelty of our study is that it analyzes not only the effects of pathological levels of hyperthyroidism on keratinocyte proliferation/differentiation balance, but it also addresses the physiological role of the D3 enzyme in the skin. Indeed, together with the brain, the skin is the only adult tissue that expresses D3 (12). What is the reason for such a specific expression profile?

Our study shows that targeted gene disruption of D3 in the epidermis critically affects the basal turnover of keratinocytes in the adult skin. D3 depletion leads to a thinner epidermis, and to enhanced expression of stratified layers and a sharp decrease in the stem cell compartment, as well as a reduction in the basal, proliferative cells. One of the consequences of the altered homeostatic balance between epidermal layers is the delayed regenerative ability of D3-depleted skin after a wound. In this scenario, massive induction of D3 expression in the early phases of regeneration may well correlate with a requirement of increased cellular proliferation. Thus, these data indicate that D3 is an essential component of the epidermal homeostatic control of keratinocyte turnover, and suggest that attenuation of TH signaling is critical for the normal physiology of a high-turnover, self-repairing and self-renewing organ such as the skin.

Hair undergoes periods of growth (anagen), regression (catagen) and rest (telogen), thereby generating and maintaining the hair cycling (33). Notably, D3 is highly expressed in anagen, thus coinciding with the highest levels of the Shh pathway which has been shown a positively regulator of D3 expression (17) and one of the well known anagen-inducing pathway (34). Since D3 is also expressed in the anagen and catagen phase of the hair follicle cycle, its depletion also alters the normal progression of the hair follicle cycle, and causes premature evolution of the hairs to the telogen phase.

Finally, disruption of the D3-mediated TH signal attenuation leads also to a drastic reduction of the number of epidermal stem cells. In the skin, a population of adult stem-cells with self-renewal capacity is located into the basal layer of the epidermis ("interfollicular epidermal stem cells") and in the bulge of the hair follicle (35). Epidermal stem cells are responsible for the epidermal renewal throughout life (36). Moreover, following an injury, the epidermal stem cells undergo amplification and the differentiation to replenish the mature epidermis in adult skin (36).

D3 expression has been shown to play critical roles in regenerative processes of different organs, such as muscle regeneration (22), liver regeneration (37) and brain repair (38). The finding that D3 depletion reduces the percentage of the epidermal stem cells reinforces the role of D3 in the regenerative capacity of the adult tissues and indicates D3 as an important source for novel therapeutic approaches in the management of wounds.

The results of this study have several important implications: (1) they reinforce previous studies indicating that the intracellular control of TH by deiodinases critically affects the balance between proliferation and differentiation (28); (2) they demonstrate that in mouse epidermis, excess of T3 accelerates the differentiation of keratinocytes, induces premature differentiation, thereby resulting in thinner epidermis; (3) indicate that TH is one of the signaling pathways regulating the spatiotemporal control of skin development and turnover; (4) establish D3 as a key determinant of the coordinated transition between anagen-to-catagen in the hair follicle cycle; (5) provide a new example of the physiological relevance of D3 in the morphogenesis, homeostatic regulation and regeneration of adult skin.

MATERIALS AND METHODS

Cell cultures.

Mouse primary keratinocytes were isolated from C57BL/6 newborn mice and cultured under low-calcium conditions (0.05 mM) in the presence of 4% calcium-chelated FBS (Invitrogen) and EGF (Invitrogen) as previously described (21). For depletion of D3 in primary culture of mouse keratinocytes, adenoviral transduction of Cre-recombinase was performed as described previously (39). Freshly isolated mouse primary

keratinocytes from K14CRE$^{ERT-/-}$; D3$^{fl/fl}$ and K14CRE$^{ERT+/-}$; D3$^{fl/fl}$ mice were incubated in suspension with control adenoviruses (Ad-IRES-GFP (Ad-GFP), Vector Biolab) or adenoviruses expressing Cre recombinase (Ad-Cre-IRES-GFP (Ad-Cre), Vector Biolab) at a multiplicity of infection (MOI) of 50 for 1 hour at 37°C. To evaluate proliferation, cells were incubated with BrdU labelling reagent (B-5002 Sigma) for 2h before of the harvest. For immunofluorescence staining, cells were fixed with 4% formaldehyde and permeabilized with 50mM NaOH, then blocked with 5% goat serum and incubated with monoclonal Ab G3G4 (Developmental Studies Hybridoma Bank) and DNase. Alexa Fluor 595–conjugated secondary antibody was used. The cell DNA was stained with 300 nM DAPI (Molecular Probes, Invitrogen).

Animals, Histology and Immunostaining

D3KO (K14Cre^{ERT}-D3$^{fl/fl}$) mice were obtained by crossing the keratinocyte-specific conditional K14Cre^{ERT} mouse (40) with D3$^{fl/fl}$ (21) mice. Depletion was induced by treatment with 10 mg of tamoxifen at different time points as indicated in each experiment. K14Cre^{ERT}-D3$^{fl/fl}$; Gt (ROSA)26Sor$^{tm4(ACTB-tdTomato,-EGFP)Luo}$ were obtained by crossing K14Cre^{ERT}-D3$^{fl/fl}$ with Gt(ROSA)26Sor$^{tm4(ACTB-tdTomato,-EGFP)Luo}$ (The Jackson Laboratory).

For immunofluorescence and histology, dorsal skin from D3KO and control mice was embedded in paraffin, cut into 7-μm sections, and H&E-stained. Slides were baked at 37°C, deparaffinized by xylenes, dehydrated with ethanol, rehydrated in PBS, and permeabilized by placing them in 0.2% Triton X-100 in PBS. Antigens were retrieved by incubation in 0.1 M citrate buffer (pH 6.0) or 0.5 M Tris buffer (pH 8.0) at 95°C for 5 min. Sections were blocked in 1% BSA/0.02% Tween/PBS for 1 hour at room temperature. Primary antibodies were incubated overnight at 4°C in blocking buffer and washed in 0.2% Tween/PBS. Secondary antibodies were incubated at room temperature for 1 hour, and washed in 0.2% Tween/PBS. Images were acquired with an IX51 Olympus microscope and the Cell*F Olympus Imaging Software.

For epidermal thickness analysis, 7 μm serial paraffin sections and stained with hematoxylin & eosin (H&E). For assessment of EdU incorporation, mice were intraperitoneally injected with 10 mg/mL EdU (Invitrogen, E10415) into the abdominal

cavity. 2 hours after EdU injection mice were euthanized and dorsal skin were formalin fixed and paraffin embedded as previously described. Immunostaining was performed with Click-iT™ EdU Cell Proliferation Kit (Thermofisher cat.number C10339).

Hair follicle cycle

Hair follicle cycle of CTR and D3KO mice was performed as previously described by (41). Briefly, dorsal back of 3-months-old anesthetised D3KO and control mice were shaved using clamp. The mice were harvested after 6 days for the anagen, 10 days for the catagen and 30 days for the telogen analysis and dorsal skin was collected for molecular and histological analysis (33).

Wound preparation, macroscopic examination and histological analyses

Skin wounds from CTR and D3KO mice were prepared as described previously (42). Briefly, mice were deeply anesthetized with ketamine. After shaving and cleaning with 70% alcohol, excisional, full-thickness skin wounds were aseptically made on the dorsal skin by picking up a fold skin at the midline and using a sterile, disposable biopsy punch with a diameter of 8 mm to punch through the two layers of skin. In this manner, two wounds were made on each side of the midline at the same time. Each wound site was digitally photographed using the Nikon FX-35A at the indicated time intervals, and wound areas were determined on photographs using Image J without a prior knowledge of the experimental procedures. Changes in wound areas were expressed as the percentage of the initial wound areas. For histological analyses of wound sites skin-wound were fixed in 4% formaldehyde buffered with phosphate-buffered saline (PBS; pH 7.2) and were then embedded with paraffin. Sections (6-µm thick) were stained with hematoxylin and eosin for histological analysis and immunofluorescence analyses for K14 were performed.

Protein Extraction from Skin and Western Blot Analysis

Dorsal skin was removed from mice and immediately snap-frozen in liquid N_2. 800 µL of lysis buffer (0.125 M Tris pH 8.6; 3% SDS, protease inhibitors including PMSF 1 mM and phosphatase inhibitors) were added to all dorsal skin samples, which were then

399 homogenized with Tissue Lyser (Qiagen). Total protein extracts from cells and from
400 skin tissue were run on a 10% SDS-PAGE gel and transferred onto an Immobilon-P
401 transfer membrane (Millipore). The membrane was then blocked with 5% non-fat dry
402 milk in PBS, probed with anti-K5, anti-Loricrin, anti-D3, anti-ERK and anti-tubulin
403 antibodies overnight at 4°C, washed, and incubated with horseradish peroxidase-
404 conjugated anti-mouse immunoglobulin G secondary antibody (1:3000), and detected
405 by chemiluminescence (Millipore, cat. WBKLS0500). After extensive washing, the
406 membrane was incubated with anti-Tubulin specific antibodies (Santa Cruz
407 Biotechnology) as loading control. All Western blots were run in triplicate, and bands
408 were quantified with ImageJ software. Antibodies and primer sequences are indicated in
409 the Supplementary section.
410
411 Real Time PCR
412 Messenger RNAs were extracted with Trizol reagent (Life Technologies Ltd).
413 Complementary DNAs were prepared with Vilo reverse transcriptase (Life
414 Technologies Ltd.) as indicated by the manufacturer. The cDNAs were amplified by
415 PCR in an iQ5 Multicolor Real Time Detector System (BioRad) with the fluorescent
416 double-stranded DNA-binding dye SYBR Green (Biorad). Specific primers for each
417 gene were designed to work under the same cycling conditions (95°C for 10 min
418 followed by 40 cycles at 95°C for 15 s and 60°C for 1 min), thereby generating products
419 of comparable sizes (about 200 bp for each amplification). Primer combinations were
420 positioned whenever possible to span an exon–exon junction and the RNA digested
421 with DNAse to avoid genomic DNA interference. Primer sequences are indicated in the
422 Supplementary section. For each reaction, standard curves for reference genes were
423 constructed based on six four-fold serial dilutions of cDNA. All samples were run in
424 triplicate. The template concentration was calculated from the cycle number when the
425 amount of PCR product passed a threshold established in the exponential phase of the
426 PCR. The relative amounts of gene expression were calculated with cyclophilin A
427 expression as an internal standard (calibrator). The results, expressed as N-fold
428 differences in target gene expression, were determined as follows: N *target = $2^{(DCt}$
429 $^{sample-DCt\ calibrator)}$. For primer sequences see supplemental Table 1.
430

Isolation of Epithelial Stem Cells

Epithelial Stem cells from D3KO and control mice were obtained as described previously (43). Immunostaining was performed using APC-anti-mouse CD34 (code 119310; Biolegend), PE-rat anti human α6-integrin (code 555736; BD Pharmingen). Fluorescence-activated cell sorting analysis was performed using FACS Canto2 software (FACS Canto2, Becton Dickinson).

Dorsal Skin was removed from mice and treated whit tripsin 0,25% over night after removal of adipose tissue. The epidermal layer was separated from derma, chopped and incubated with tripsin 0,25% for 7 minutes to 37°C. After digestion, FBS was added to sample to inactivate tripsin. The cells were filtered with 70μm cell strainer. Immunostaining was performed using APC-anti-mouse CD34 (cod 119310;Biolegend), PE-rat anti human α6-integrin (cod 555736; BD Pharmingen), by incubation for 1 hour RT. Fluorescence-activated cell sorting analysis was performed using FACS Canto2 software (FACS Canto2, Becton Dickinson).

T4 Clearance experiment.

8 week old mice were intraperitoneally (i.p.) injected with 20 μg/100g of T4. Starting one day before injection, the blood was collected by retro-orbital withdrawal at 24 and 48 hours after a single T4 injection. The serums were separated and the determination of T4 was measured by Rodent T4 Elisa Test Kit (Endocrine Technologies Inc. USA). Experiments were performed with 6 mice per group and repeated two times in these conditions.

Statistics

The results are shown as means ± SD throughout. Differences between samples were assessed by the Student's two-tailed t test for independent samples. Relative mRNA levels (in which the control sample was arbitrarily set as 1) are reported as results of real time PCR, in which the expression of cyclophilin A served as housekeeping gene. In all experiments, differences were considered significant when p was less than 0.05. Asterisks indicate significance at $*P < 0.05$, $**P < 0.01$, and $***P < 0.001$ throughout.

Acknowledgments

This work was supported by grants from AIRC to M.D. (IG 13065), by the ERCStG2014 grant from European Research Council under the European Union's Horizon2020 Programme (STARS – 639548), by the EU FP7 contract Thyrage (grant number 666869) to M.D. and by the grant FARE from MIUR (R16KPLYF38) to M.D. The authors have declared that no conflict of interest exists. We thank Jean Ann Gilder (Scientific Communication srl., Naples, Italy) for writing assistance.

Author contributions

G.M., A.S., C.L., E.D.C., C.M., A.G.C., A.N., S.S., M.A.D.S. and D.D.G performed *in vitro* and *in vivo* experiments and prepared figures; R.A. generated plasmids and mouse models; F.V. performed FACS analysis studies; M.D. designed the overall study, supervised the experiments, analyzed the results, and wrote the paper; and all authors discussed the results and provided input on the manuscript.

REFERENCES

1. Fuchs E, and Raghavan S. Getting under the skin of epidermal morphogenesis. *Nat Rev Genet.* 2002;3(3):199-209.
2. Dai X, and Segre JA. Transcriptional control of epidermal specification and differentiation. *Curr Opin Genet Dev.* 2004;14(5):485-91.
3. Moll R, Divo M, and Langbein L. The human keratins: biology and pathology. *Histochem Cell Biol.* 2008;129(6):705-33.
4. Fuchs E, and Green H. Changes in keratin gene expression during terminal differentiation of the keratinocyte. *Cell.* 1980;19(4):1033-42.
5. Antonini D, Sibilio A, Dentice M, and Missero C. An Intimate Relationship between Thyroid Hormone and Skin: Regulation of Gene Expression. *Front Endocrinol (Lausanne).* 2013;4:104.
6. Safer JD. Thyroid hormone and wound healing. *J Thyroid Res.* 2013;2013:124538.
7. Slominski A, Wortsman J, Kohn L, Ain KB, Venkataraman GM, Pisarchik A, et al. Expression of hypothalamic-pituitary-thyroid axis related genes in the human skin. *J Invest Dermatol.* 2002;119(6):1449-55.
8. Paus R. Exploring the "thyroid-skin connection": concepts, questions, and clinical relevance. *J Invest Dermatol.* 2010;130(1):7-10.

9. Horsley V. The Brown Lectures on Pathology. *Br Med J.* 1885;1(1255):111-5.
10. Luongo C, Dentice M, and Salvatore D. Deiodinases and their intricate role in thyroid hormone homeostasis. *Nat Rev Endocrinol.* 2019;15(8):479-88.
11. Cicatiello AG, Ambrosio R, and Dentice M. Thyroid hormone promotes differentiation of colon cancer stem cells. *Mol Cell Endocrinol.* 2017;459:84-9.
12. Dentice M, and Salvatore D. Deiodinases: the balance of thyroid hormone: local impact of thyroid hormone inactivation. *J Endocrinol.* 2011;209(3):273-82.
13. Huang SA, Dorfman DM, Genest DR, Salvatore D, and Larsen PR. Type 3 iodothyronine deiodinase is highly expressed in the human uteroplacental unit and in fetal epithelium. *J Clin Endocrinol Metab.* 2003;88(3):1384-8.
14. Huang SA. Physiology and pathophysiology of type 3 deiodinase in humans. *Thyroid.* 2005;15(8):875-81.
15. Peeters RP, Wouters PJ, Kaptein E, van Toor H, Visser TJ, and Van den Berghe G. Reduced activation and increased inactivation of thyroid hormone in tissues of critically ill patients. *J Clin Endocrinol Metab.* 2003;88(7):3202-11.
16. Olivares EL, Marassi MP, Fortunato RS, da Silva AC, Costa-e-Sousa RH, Araujo IG, et al. Thyroid function disturbance and type 3 iodothyronine deiodinase induction after myocardial infarction in rats a time course study. *Endocrinology.* 2007;148(10):4786-92.
17. Dentice M, Luongo C, Huang S, Ambrosio R, Elefante A, Mirebeau-Prunier D, et al. Sonic hedgehog-induced type 3 deiodinase blocks thyroid hormone action enhancing proliferation of normal and malignant keratinocytes. *Proc Natl Acad Sci U S A.* 2007;104(36):14466-71.
18. Dentice M, Luongo C, Ambrosio R, Sibilio A, Casillo A, Iaccarino A, et al. beta-Catenin regulates deiodinase levels and thyroid hormone signaling in colon cancer cells. *Gastroenterology.* 2012;143(4):1037-47.
19. Huang SA, Tu HM, Harney JW, Venihaki M, Butte AJ, Kozakewich HP, et al. Severe hypothyroidism caused by type 3 iodothyronine deiodinase in infantile hemangiomas. *N Engl J Med.* 2000;343(3):185-9.
20. Nauman P, Bonicki W, Michalik R, Warzecha A, and Czernicki Z. The concentration of thyroid hormones and activities of iodothyronine deiodinases are altered in human brain gliomas. *Folia Neuropathol.* 2004;42(2):67-73.
21. Di Girolamo D, Ambrosio R, De Stefano MA, Mancino G, Porcelli T, Luongo C, et al. Reciprocal interplay between thyroid hormone and microRNA-21 regulates hedgehog pathway-driven skin tumorigenesis. *J Clin Invest.* 2016;126(6):2308-20.
22. Dentice M, Ambrosio R, Damiano V, Sibilio A, Luongo C, Guardiola O, et al. Intracellular inactivation of thyroid hormone is a survival mechanism for muscle stem cell proliferation and lineage progression. *Cell Metab.* 2014;20(6):1038-48.

544 23. Huelsken J, Vogel R, Erdmann B, Cotsarelis G, and Birchmeier W. beta-
545 Catenin controls hair follicle morphogenesis and stem cell differentiation in
546 the skin. *Cell.* 2001;105(4):533-45.
547 24. Brancati F, Fortugno P, Bottillo I, Lopez M, Josselin E, Boudghene-Stambouli
548 O, et al. Mutations in PVRL4, encoding cell adhesion molecule nectin-4,
549 cause ectodermal dysplasia-syndactyly syndrome. *Am J Hum Genet.*
550 2010;87(2):265-73.
551 25. Szegedi A, Payer E, Czifra G, Toth BI, Schmidt E, Kovacs L, et al. Protein
552 kinase C isoenzymes differentially regulate the differentiation-dependent
553 expression of adhesion molecules in human epidermal keratinocytes. *Exp*
554 *Dermatol.* 2009;18(2):122-9.
555 26. Yang M, Song S, Dong K, Chen X, Liu X, Rouzi M, et al. Skin transcriptome
556 reveals the intrinsic molecular mechanisms underlying hair follicle cycling
557 in Cashmere goats under natural and shortened photoperiod conditions. *Sci*
558 *Rep.* 2017;7(1):13502.
559 27. Dotto GP. Signal transduction pathways controlling the switch between
560 keratinocyte growth and differentiation. *Crit Rev Oral Biol Med.*
561 1999;10(4):442-57.
562 28. Dentice M, Marsili A, Zavacki A, Larsen PR, and Salvatore D. The deiodinases
563 and the control of intracellular thyroid hormone signaling during cellular
564 differentiation. *Biochim Biophys Acta.* 2013;1830(7):3937-45.
565 29. Sagliocchi S, Cicatiello AG, Di Cicco E, Ambrosio R, Miro C, Di Girolamo D, et
566 al. The thyroid hormone activating enzyme, type 2 deiodinase, induces
567 myogenic differentiation by regulating mitochondrial metabolism and
568 reducing oxidative stress. *Redox Biol.* 2019;24:101228.
569 30. Contreras-Jurado C, Garcia-Serrano L, Martinez-Fernandez M, Ruiz-Llorente
570 L, Paramio JM, and Aranda A. Impaired hair growth and wound healing in
571 mice lacking thyroid hormone receptors. *PLoS One.* 2014;9(9):e108137.
572 31. Furlow JD, and Neff ES. A developmental switch induced by thyroid
573 hormone: Xenopus laevis metamorphosis. *Trends Endocrinol Metab.*
574 2006;17(2):40-7.
575 32. Leonhardt JM, and Heymann WR. Thyroid disease and the skin. *Dermatol*
576 *Clin.* 2002;20(3):473-81, vii.
577 33. Stenn KS, and Paus R. Controls of hair follicle cycling. *Physiol Rev.*
578 2001;81(1):449-94.
579 34. Sato N, Leopold PL, and Crystal RG. Induction of the hair growth phase in
580 postnatal mice by localized transient expression of Sonic hedgehog. *J Clin*
581 *Invest.* 1999;104(7):855-64.
582 35. Blanpain C, Lowry WE, Geoghegan A, Polak L, and Fuchs E. Self-renewal,
583 multipotency, and the existence of two cell populations within an epithelial
584 stem cell niche. *Cell.* 2004;118(5):635-48.
585 36. Mascre G, Dekoninck S, Drogat B, Youssef KK, Brohee S, Sotiropoulou PA, et
586 al. Distinct contribution of stem and progenitor cells to epidermal
587 maintenance. *Nature.* 2012;489(7415):257-62.

588 37. Kester MH, Toussaint MJ, Punt CA, Matondo R, Aarnio AM, Darras VM, et al.
589 Large induction of type III deiodinase expression after partial hepatectomy
590 in the regenerating mouse and rat liver. *Endocrinology.* 2009;150(1):540-5.
591 38. Li WW, Le Goascogne C, Ramauge M, Schumacher M, Pierre M, and Courtin
592 F. Induction of type 3 iodothyronine deiodinase by nerve injury in the rat
593 peripheral nervous system. *Endocrinology.* 2001;142(12):5190-7.
594 39. LaMarca HL, Visbal AP, Creighton CJ, Liu H, Zhang Y, Behbod F, et al.
595 CCAAT/enhancer binding protein beta regulates stem cell activity and
596 specifies luminal cell fate in the mammary gland. *Stem Cells.*
597 2010;28(3):535-44.
598 40. Lapouge G, Beck B, Nassar D, Dubois C, Dekoninck S, and Blanpain C. Skin
599 squamous cell carcinoma propagating cells increase with tumour
600 progression and invasiveness. *EMBO J.* 2012;31(24):4563-75.
601 41. Plikus MV, and Chuong CM. Complex hair cycle domain patterns and
602 regenerative hair waves in living rodents. *J Invest Dermatol.*
603 2008;128(5):1071-80.
604 42. Mori R, Kondo T, Ohshima T, Ishida Y, and Mukaida N. Accelerated wound
605 healing in tumor necrosis factor receptor p55-deficient mice with reduced
606 leukocyte infiltration. *FASEB J.* 2002;16(9):963-74.
607 43. Nowak JA, and Fuchs E. Isolation and culture of epithelial stem cells.
608 *Methods Mol Biol.* 2009;482:215-32.
609

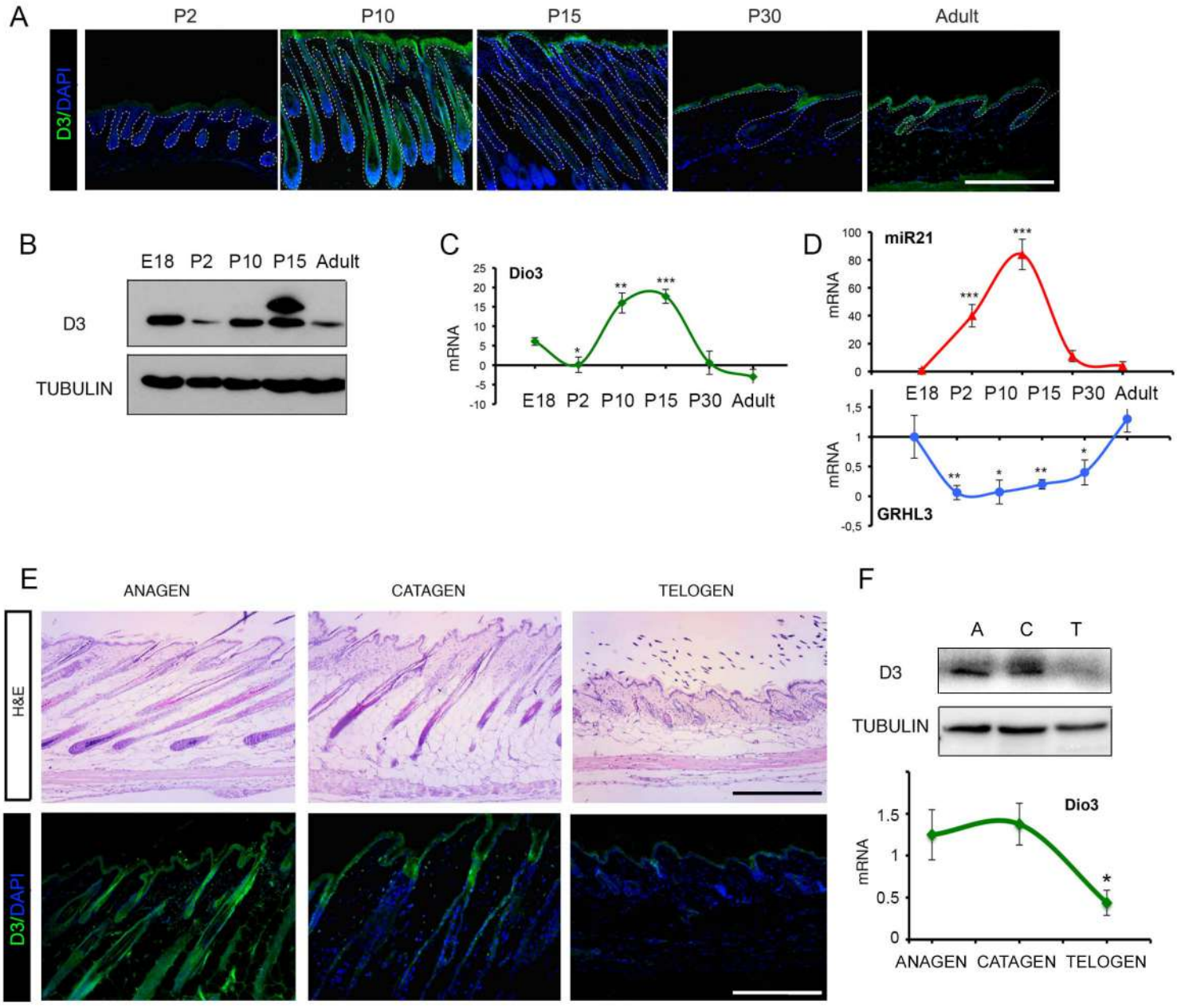
A
P2
P10
P15
P30
Adult
D3/DAPI
B
E18 P2 P10 P15 Adult
D3
TUBULIN
C
Dio3
mRNA
E18 P2 P10 P15 P30 Adult
D
miR21
mRNA
E18 P2 P10 P15 P30 Adult
GRHL3
E
ANAGEN
CATAGEN
TELOGEN
H&E
D3/DAPI
F
A C T
D3
TUBULIN
Dio3
mRNA
ANAGEN CATAGEN TELOGEN

Figure 1

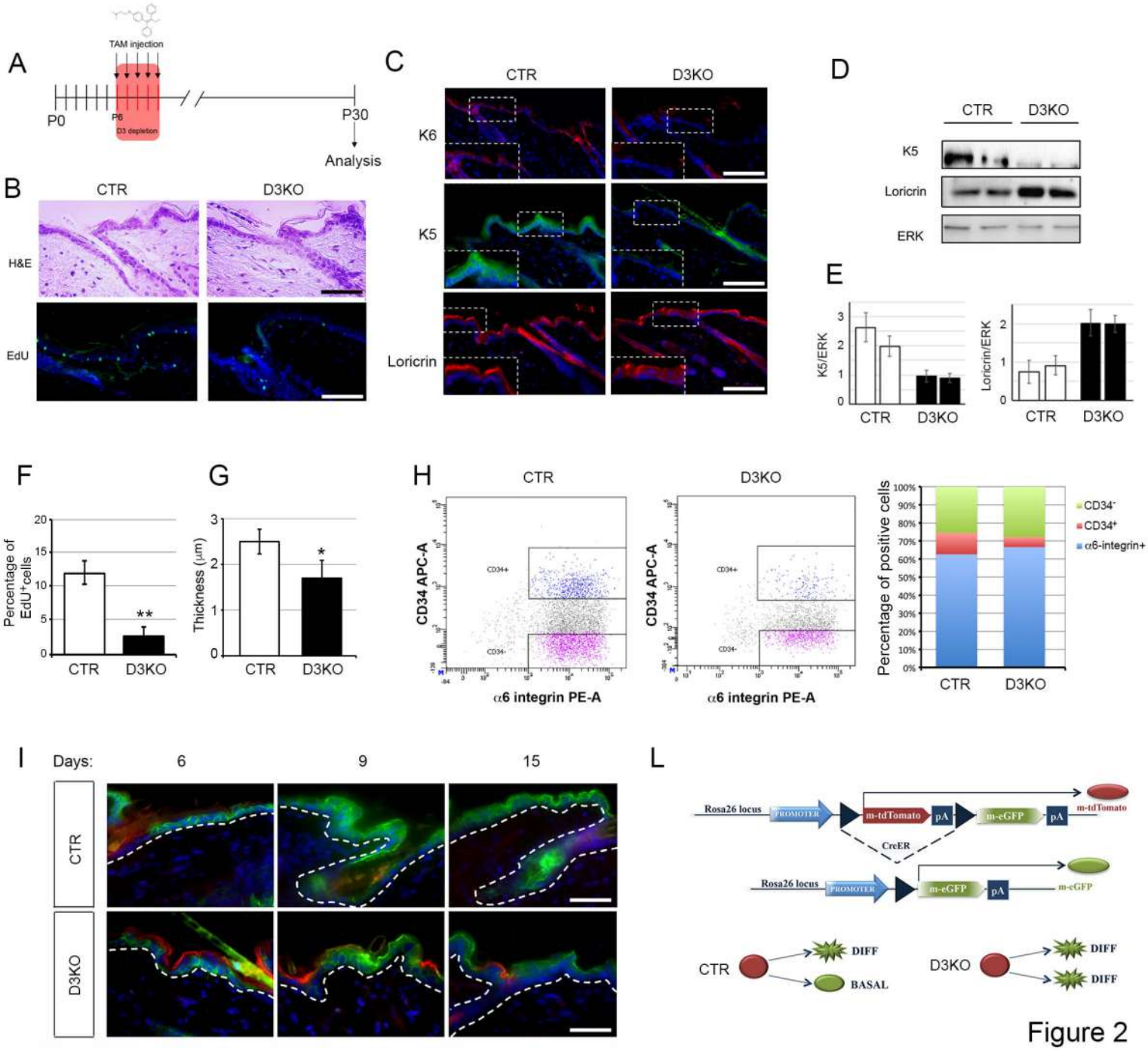
A
TAM injection
P0
P6
D3 depletion
P30
Analysis
B
CTR
D3KO
H&E
EdU
C
CTR
D3KO
K6
K5
Loricrin
D
CTR
D3KO
K5
Loricrin
ERK
E
K5/ERK
Loricrin/ERK
CTR
D3KO
F
Percentage of EdU+cells
**
G
Thickness (μm)
*
H
CTR
D3KO
CD34 APC-A
α6 integrin PE-A
CD34+
CD34-
Percentage of positive cells
CD34-
CD34+
α6-integrin+
I
Days:
6
9
15
CTR
D3KO
L
Rosa26 locus
PROMOTER
m-tdTomato
pA
m-eGFP
CreER
DIFF
BASAL

Figure 2

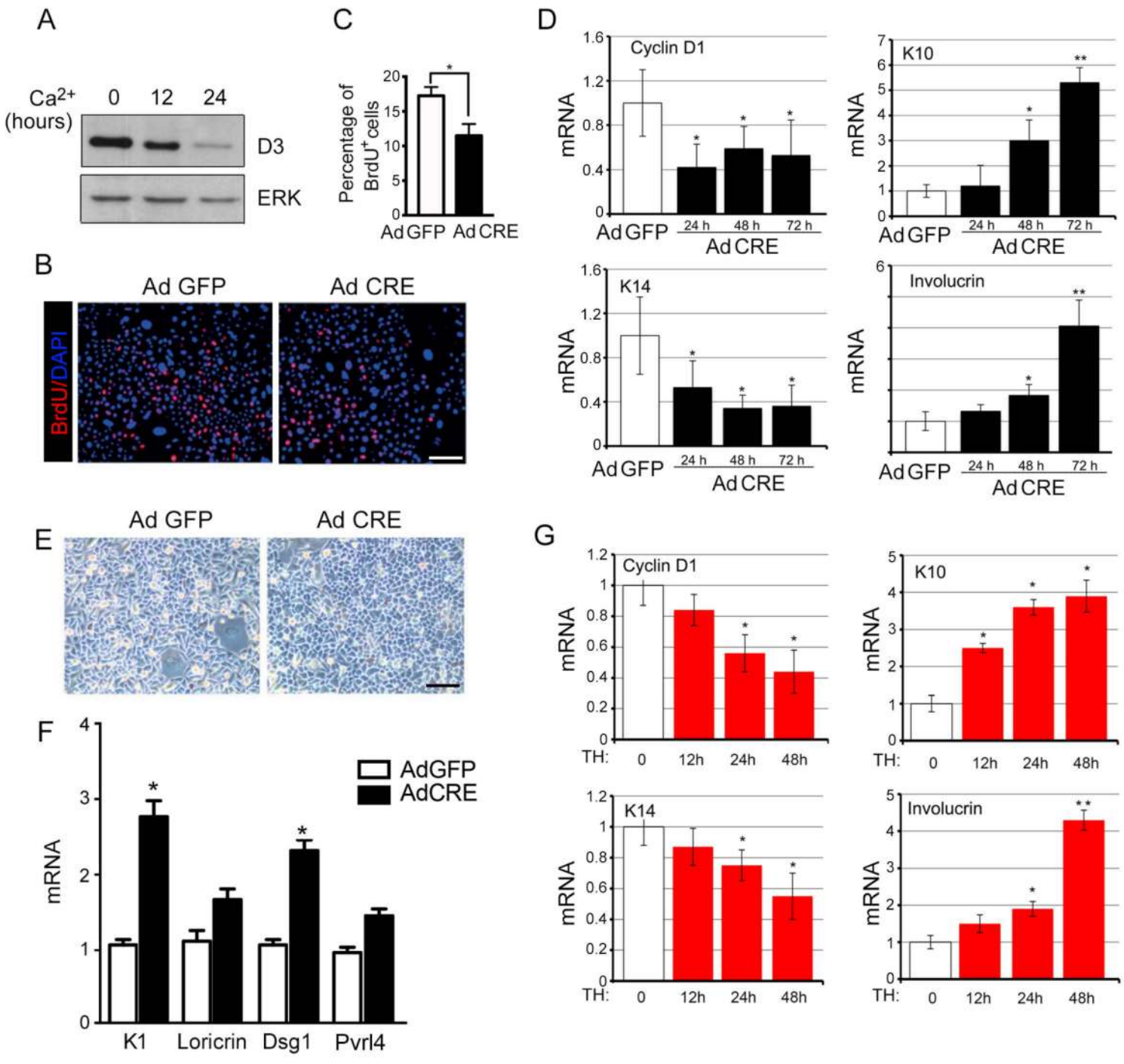
A
Ca2+ (hours)
0
12
24
D3
ERK
C
Percentage of BrdU+ cells
Ad GFP
Ad CRE
B
Ad GFP
Ad CRE
BrdU/DAPI
D
Cyclin D1
K10
K14
Involucrin
mRNA
Ad GFP
24 h
48 h
72 h
Ad CRE
E
Ad GFP
Ad CRE
F
AdGFP
AdCRE
mRNA
K1
Loricrin
Dsg1
Pvrl4
G
Cyclin D1
K10
K14
Involucrin
mRNA
TH:
0
12h
24h
48h

Figure 3

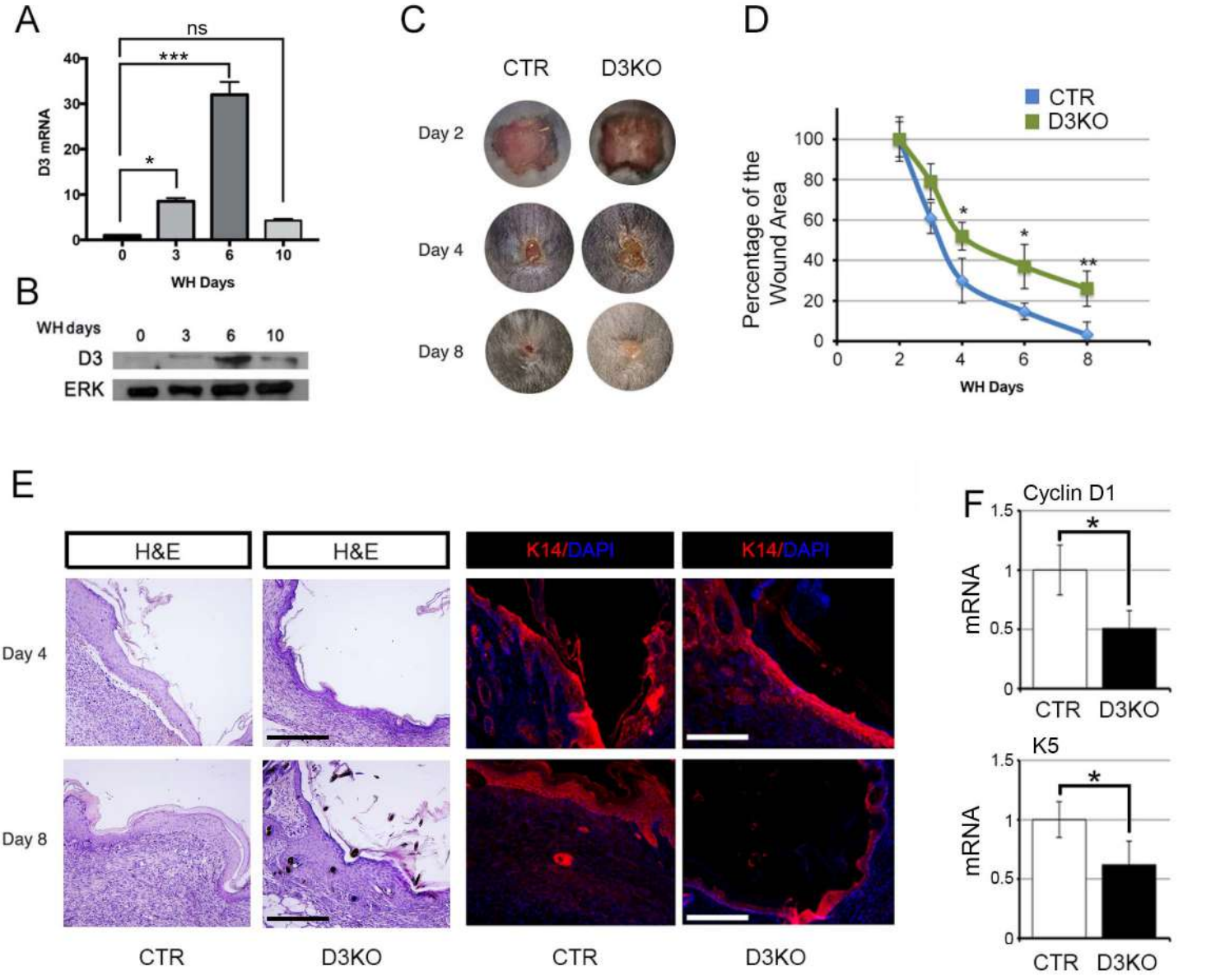
A
ns
***
*
D3 mRNA
40
30
20
10
0
0
3
6
10
WH Days
B
WH days
0
3
6
10
D3
ERK
C
CTR
D3KO
Day 2
Day 4
Day 8
D
CTR
D3KO
Percentage of the Wound Area
100
80
60
40
20
0
0
2
4
6
8
WH Days
*
*
**
E
H&E
H&E
K14/DAPI
K14/DAPI
Day 4
Day 8
CTR
D3KO
CTR
D3KO
F
Cyclin D1
mRNA
1.5
1
0.5
0
*
CTR
D3KO
K5
mRNA
1.5
1
0.5
0
*
CTR
D3KO
G
BrdU
K14
BrdU/K14/DAPI
50um
CTR
200 um
BrdU
K14
BrdU/K14/DAPI
50 um
D3KO
200 um
H
Percentage of BrdU+ cells
30
20
10
0
*
CTR
D3KO

Figure 4

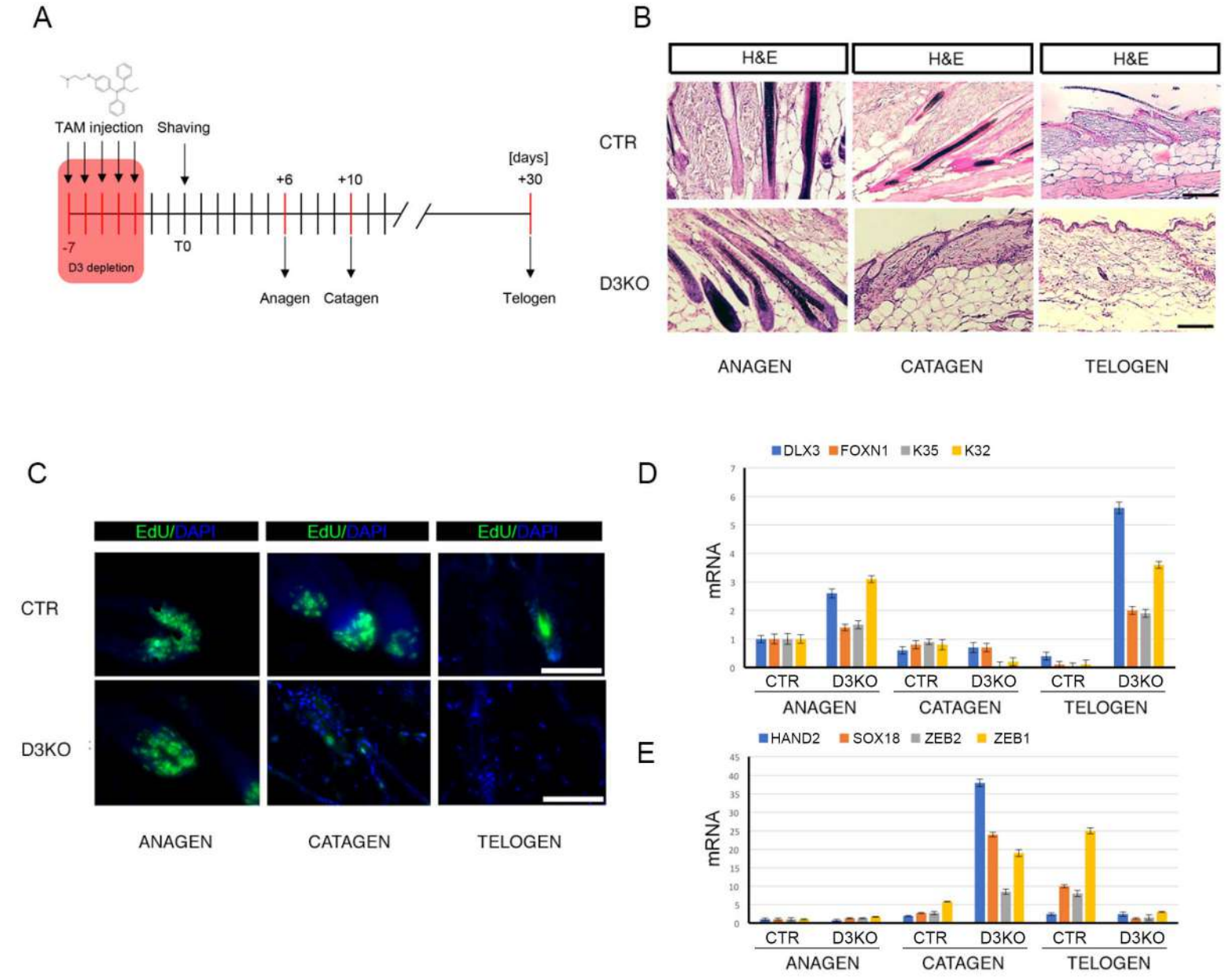
A
TAM injection
Shaving
[days]
+6
+10
+30
-7
D3 depletion
T0
Anagen
Catagen
Telogen
B
H&E
H&E
H&E
CTR
D3KO
ANAGEN
CATAGEN
TELOGEN
C
EdU/DAPI
EdU/DAPI
EdU/DAPI
CTR
D3KO
ANAGEN
CATAGEN
TELOGEN
D
DLX3
FOXN1
K35
K32
mRNA
CTR
D3KO
CTR
D3KO
CTR
D3KO
ANAGEN
CATAGEN
TELOGEN
E
HAND2
SOX18
ZEB2
ZEB1
mRNA
CTR
D3KO
CTR
D3KO
CTR
D3KO
ANAGEN
CATAGEN
TELOGEN

Figure 5

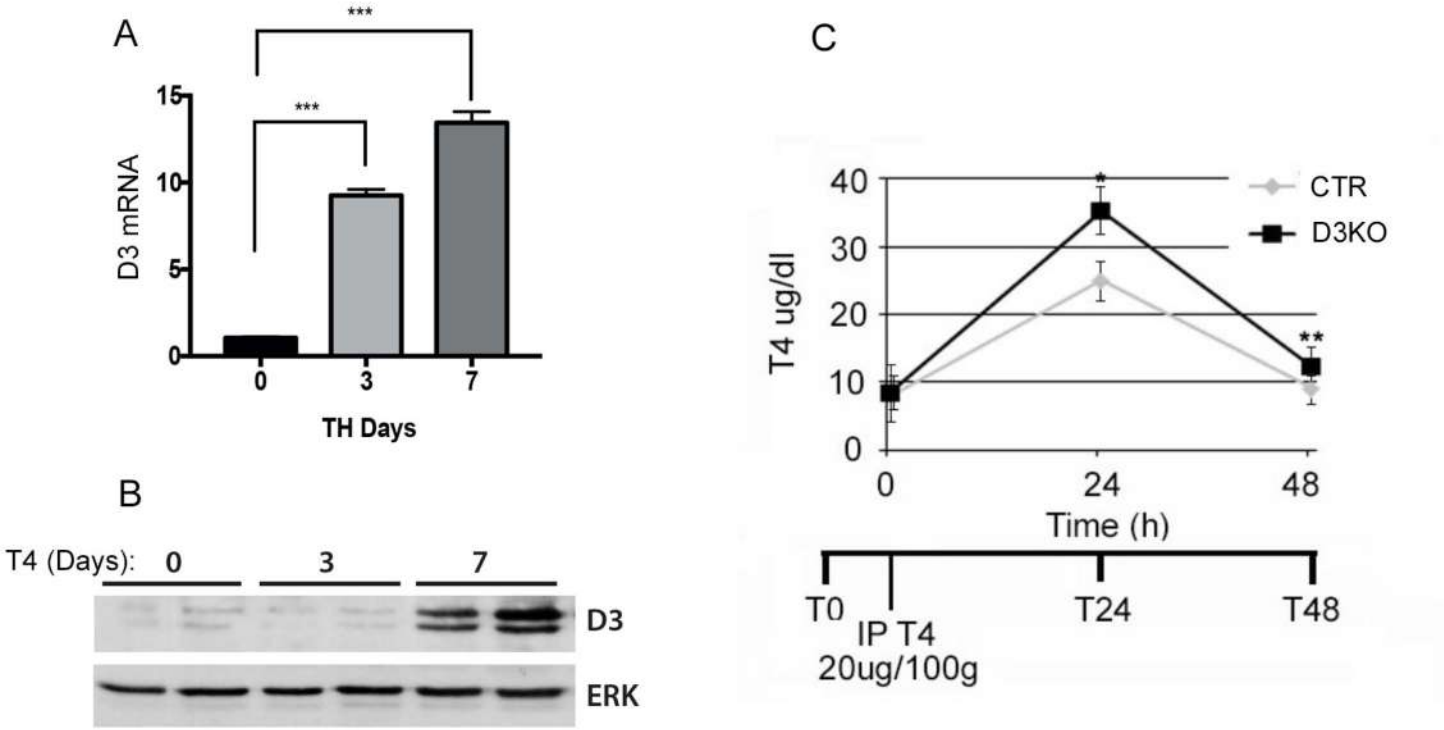
A
***
***
15
10
5
0
D3 mRNA
0
3
7
TH Days
B
T4 (Days): 0
3
7
D3
ERK
C
40
30
20
10
0
T4 ug/dl
CTR
D3KO
*
**
0
24
48
Time (h)
T0
IP T4
20ug/100g
T24
T48

Figure 6

FIGURE LEGENDS

Figure 1. *Type 3 deiodinase is dynamically expressed in adult epidermis and hair follicle cycle.* **(A)** D3 expression was assessed by immunofluorescence at different postnatal days and in the adult epidermis. Scale bars represent 200 μm**. (B)** Western blot analysis of D3 protein expression as in A. **(C-D)** mRNA expression profile of D3, miR21 and GRHL3 during epithelial ontogenesis. **(E-F)** Expression of D3 in the hair follicle cycle was analysed by immunofluorescence, western blot and real time PCR in 3 months old mice. Scale bars represents 200 μm**.** Data are shown as average ± SD. *$P < 0.05$, **$P < 0.01$, ***$P < 0.001$.

Figure 2. *Genetic depletion of D3 in the epidermis reduces the thickness of the skin and increases the expression of differentiative markers.* **(A)** Schematic representation of experimental protocol for D3 depletion in skin compartment by tamoxifen treatment. **(B)** Hematoxilin and eosin (H&E) staining and immunofluorescence for EdU was performed in 3 months old of control and D3KO mice. **(C)** Expression of the proliferative marker K6, the basal layer K5 and the differentiative marker Loricrin were assessed by immunofluorescence in the same mice as in B. **(D-E)** K5 and Loricrin expression were measured by western blot analysis. Tubulin expression was evaluated as loading control. **(F)** EdU-positive cells were measured as indicated in methods in the same samples as in B. **(G)** Thickness of the epidermis was measured as indicated in methods in the same samples as in B. **(H)** Measurement of the percentage of $CD34^+$ stem cells in control and D3KO mice was performed by FACS sorting analysis in 3 old months mice. The relative percentage of α6-integrin positive cells (representing the total amounts of epithelial cells), $CD34^-$ and $CD34^+$ cells is represented by graph bars. **(I)** Tomato/GFP mice; CTR and Tomato/GFP mice; D3KO mice were induced by tamoxifen treatment and the localization of green cells was analyzed by fluorescence at 6, 9 and 15 days following treatment. **(L)** Schematic representation of the tamoxifen-induced Tomato/GFP recombination and proposed model of the balance between proliferation and differentiation in control and D3KO mice. Data are shown as average ± SD. *$P < 0.05$.

Figure 3. *In vitro depletion of D3 and treatment with T3 accelerates differentiation and reduces proliferation of mouse keratinocytes.* **(A)** Primary cultures of mouse keratinocytes were induced to cell differentiation as indicated in methods and harvested at 12 and 24 hours following induction of Ca^{2+}-differentiation. D3 protein levels were then measured by western blot analysis and the ERK levels were measured for loading control. **(B, C)** Freshly isolated primary keratinocytes were infected with an adenovirus overexpressing the CRE recombinase (AdCRE) or a control adenovirus

(AdGFP). 48 hours following infection, cells were fixed for immunofluorescent staining with anti-BrdU antibody. Percentage of BrdU-labeled nuclei was evaluated as BrdU+ nuclei/Tot nuclei. n = 50 fields, $P < 0.01$. **(D)** mRNA expression of genes implicated in the differentiation of keratinocytes (K10 and involucrin) or proliferation (Cycline D1) and the pan-keratin marker K14 was measured by real time PCR in primary culture of keratinocytes from control and D3KO mice. D3 depletion was induced by infection of keratinocytes with an adenovirus carrying the CRE Recombinase expression or with a GFP-expressing control adenovirus as indicated in methods. **(E)** Morphology of AdCRE and AdGFP primary mouse keratinocytes cultured in low calcium conditions (Scale bar: 100um). **(F)** K1, Loricrin, Dsg1 and Pvlr4 mRNA expression levels were measured in AdCRE and AdGFP keratinocytes. **(G)** Expression of differentiation and proliferation markers was measured by real time PCR in primary culture of keratinocytes treated or not with 30 nM T3 for the indicated times. Data are shown as average ± SD. $*P < 0.05$, $**P < 0.01$, $***P < 0.001$.

Figure 4. *D3KO mice have delayed epidermal regeneration.* **(A)** D3 mRNA expression during wound healing was measured by real time PCR analysis. The wounds were excised including 2mm of the epidermal margins for RNA isolation, at 3, 6, 10 days after injury. Cyclophilin A was used as internal control. Normalized copies of the target gene in adult healthy skin were set as 1 and it corresponds at day 0. Data are shown as average of 3 separate experiments analyzing 4 mice for each group. **(B)** Western Blot analysis was performed using our anti-D3 antibody and anti-Total ERK as loading control. **(C)** Wound Healing (WH) experiment was performed in 3 months old control and D3KO mice. Wound repair was assessed at 2, 4 and 8 days following the injury. Images are shown as representation of 3 separate experiments analyzing 4 mice for each group. **(D)** Closure of the wound area was measures as indicated in methods. **(E)** H&E and K14 immunofluorescence analysis of the repairing area at day 4 and 8 following injury. **(F)** Expression of K5 and Cyclin D1 was measured by real time PCR in the skin of repairing area at 4 days following the injury. **(G, H)** Immunofluorescent staining for BrdU positive nuclei and K14 protein (used as control of analyzed epidermal area) in sections of skin at 4 days from injury in D3KO vs control mice. The quantization of the proliferation rate is showed in graph as measure of BrdU+ nuclei/Total nuclei and was repeated in three independent experiments (4 animals for group). Values represent mean ± SEM. *, $p< 0.01$, $*P < 0.05$.

Figure 5. *Hair follicle cycle is accelerated in D3KO mice.* **(A)** Schematic representation of the tamoxifen-induced D3-depletion and the hair follicle cycle induction. **(B)** H&E staining of the dorsal skin of control and D3KO mice at the different phases of the hair follicle cycle. **(C)** EdU

staining of the same samples as in B. **(D, E)** mRNA expression of a panel of anagen (D) and telogen (E) markers was measured in dorsal skin from control and D3KO mice at the different phases of the hair follicle cycle. Expression of each gene in the anagen of the control mice was arbitrarily set as 1. *$P < 0.05$, **$P < 0.01$.

Figure 6. *D3KO mice have reduced T4 clearance.* **(A, B)** D3 mRNA and protein levels were measured by real time PCR and western blot in dorsal skin of wild type mice injected with supraphysiological dose (20 μg/100g body weight) of T4 for 3 and 7 days. **(C)** Serum T4 concentrations were measured as indicated in the Methods at different times after the intraperitoneal administration of T4. T4 serum levels were represented in relation to the first point of curve (T0, before the T4 injection). (Bottom) Schematic representation of the experimental design. Data are shown as average of 2 separate experiments analyzing 6 mice for each group. *$P < 0.05$, **$P < 0.01$.

SUPPLEMENTAL FIGURE LEGENDS

Figure S1. *D3 is expressed in embryonic epidermis from the embryonic 13.5 day and peaks at 17.5.* Immunofluorescence analysis of D3 expression at different embryonic stages.

Figure S2. *D3 is expressed in the epidermal layers and in the hair follicle of mouse skin*. Paraffin sections of adult mouse skin were probed with D3 antibody. D3 was highly expressed in the bulge, sebaceous gland of hair follicle, but it is absent from the dermal papilla.

Figure S3. *Generation of the K14-Cre^{ERT}/D3$^{Fl/Fl}$ mouse.* **(A)** K14CRE^{ERT} mice were crossed with *D3$^{Fl/Fl}$* mice to obtain the *K14-Cre^{ERT}/D3$^{Fl/Fl}$* mice. **(B)** PCR analysis demonstrated that the recombination generating the depletion of D3 is present only in the skin compartment. **(C)** Immunofluorescence analysis demonstrates the depletion of D3 protein from the epidermis in mice 10 days old (P10).

Figure S4. *Systemic thyroid status is not affected by epidermal D3 depletion.* **(A)** Serum T3, T4 and rT3 were measured by HPLC-MS in 3 months old D3KO and CTR mice (n= 6). Values are expressed as percentage of total THs. **(B)** TSH levels in serum from D3KO and CTR mice were measured by ELISA in the same mice as in A.

Figure S5. *Wound healing is delayed in D3KO mice.* Representative images of whole wound area

in D3KO and control mice at 4 and 8 days upon injury as also shown in Figure 4E.